

PicoSAM2: Low-Latency Segmentation In-Sensor for Edge Vision Applications

Pietro Bonazzi^{*†}, Nicola Farronato^{*†‡}, Stefan Zihlmann^{*†}, Haotong Qin[†], Michele Magno[†]

[†]ETH Zürich [‡]IBM Research - Zürich

Abstract—Real-time, on-device segmentation is critical for latency-sensitive and privacy-aware applications like smart glasses and IoT devices. We introduce PicoSAM2, a lightweight (1.3M parameters, 336M MACs) promptable visual segmentation model optimized for edge and in-sensor execution, including the Sony IMX500. It builds on a depthwise separable U-Net, with knowledge distillation and fixed-point prompt encoding to learn from the Segment Anything Model 2 (SAM2). On COCO and LVIS, it achieves 51.9% and 44.9% mIoU, respectively. The quantized model (1.22MB) runs at 14.3ms on the IMX500—achieving 86 MACs/cycle making it the only model meeting both memory and compute constraints for in-sensor deployment. Distillation boosts LVIS performance by +3.5% mIoU and +5.1% mAP. These results demonstrate that efficient, promptable segmentation is feasible directly on-camera, enabling privacy-preserving vision without cloud or host processing.

FUNDING & ACKNOWLEDGMENTS

This research was funded by Swiss National Science Foundation (Grant 219943), and the European Union’s HORIZON-MSCA-2022-DN-01 (Grant 101119554).

I. INTRODUCTION

Recent advances in task-agnostic segmentation, such as Meta’s Segment Anything Model (SAM) [1] and its successor SAM2 [2], enable high-quality prompt-based segmentation in various visual tasks. While SAM2 [2] improves accuracy, efficiency, and supports video input, its large size and transformer-based architecture make it unsuitable for deployment in latency and power constrained settings like smart cameras, wearable glasses, battery-operated device for the Internet of Things and drones.

Edge computing offers a solution by enabling low-latency, private inference directly on-device [3]–[6]. Recent advances in smart sensors are driving a shift toward in-sensor intelligence, enabling real-time perception directly at the point of capture. A novel sensor realized by Sony, the IMX500 camera sensor [7]–[9] integrates a camera with an edge AI processor [10], enabling real-time AI at the sensor level. However, strict hardware constraints, including a total model size below 8 MB and limited ONNX operator support, render existing promptable segmentation models, including TinySAM [11], EdgeSAM [12], MobileSAMv2 [13], and LiteSAM [14] undeployable directly on the IMX500. In fact, these models either exceed memory limits, rely on unsupported operators,

^{*}These authors contributed equally to this work.

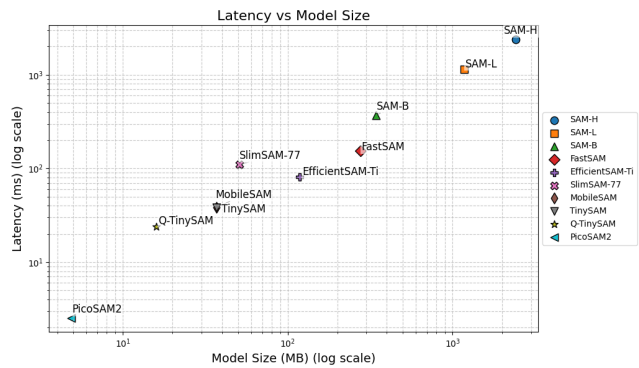


Fig. 1: Comparison of segmentation models: Latency vs. Memory

or require architectural components (e.g., transformers) incompatible with the IMX500’s execution engine.

This paper addresses the limitations mentioned above by introducing PicoSAM2 (see Figure 3), the first segmentation model to demonstrate practical in-sensor deployment designed for resource-constrained edge platforms.

II. RELATED WORK

Promptable visual segmentation has recently seen rapid advancement, with efforts focused on efficient training [14], [15], knowledge distillation [11], [12], [16]–[20], model pruning [21], and training-free methods [22] to enable efficient architectures [23] that make powerful models like SAM [1] deployable on edge devices. TinySAM [11] distills SAM into a smaller and faster model via stage-wise supervision and prompt sampling, followed by post-training quantization [24], [25]. Our work builds on this by adopting a fully custom U-Net-style student without relying on the original TinySAM backbone. EdgeSAM [12] replaces the SAM transformer encoder with a CNN, achieving over 30 FPS on mobile devices. Their “prompt-in-the-loop” distillation iteratively refines student masks with feedback prompts. In contrast, our approach encodes fixed prompt behavior statically, eliminating run-time prompt overhead. SAM2 [2] generalizes prompt segmentation to video using a pyramid transformer backbone [26]. We draw inspiration from its architecture while focusing exclusively on static images and remove temporal components to enable lightweight deployment. MobileSAMv2 [13] optimizes the SAM decoder by reducing the prompt complexity and simpli-

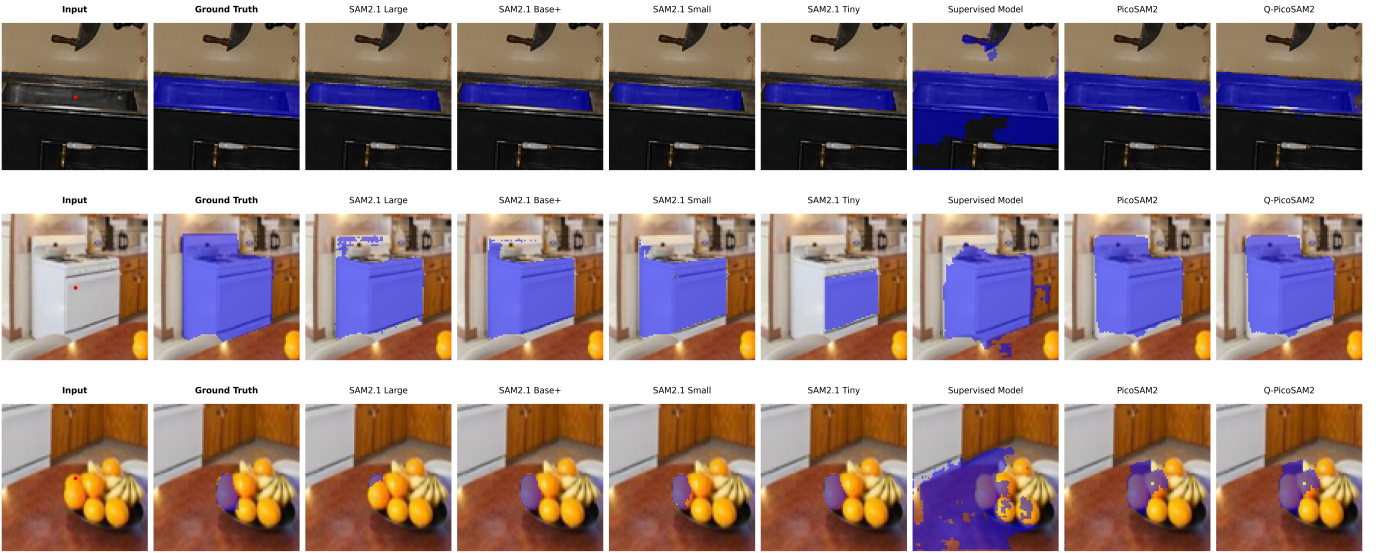


Fig. 2: Qualitative comparison of each model’s mask inference.

fyng the architecture. Similarly, we redesign the decoder using CNN-based mask heads and avoid expensive attention-based modules. LiteSAM [14] demonstrates high performance with lightweight modular components, including a transformer-based LiteViT encoder [27] and AutoPPN [28]. Although effective, its reliance on transformer blocks limits its suitability for MCU deployment. Instead, we propose a dense CNN backbone with pyramid features to mimic transformer-like capacity in-sensor [7], [8].

III. METHODOLOGY

Adapting the high-performance SAM2 model for edge and in-sensor inference—such as on the Sony IMX500 [7]—presents three key challenges: a strict 8MB memory limit, restricted ONNX operator support, and RGB-only input that excludes multimodal prompting. This paper proposes and evaluates a novel segmentation design to address these constraints.

A. Model Architecture

We designed a lightweight U-Net [29] with separable convolutions in depth [30], skip connections, and up/down sampling ensuring spatial preservation and quantization-friendliness.

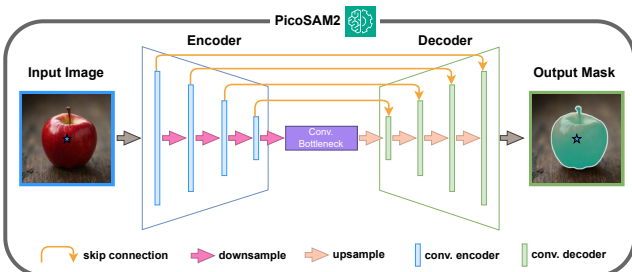


Fig. 3: Schematic of the PicoSAM2 architecture.

We cannot allow any input channels beyond RGB, which prevents explicit prompt encoding. To address this, we crop each training image so the prompt point appears at the center, allowing the model to learn a spatial prior. This implicit encoding makes the model promptable without extra input. The student learns from a teacher with full prompts while seeing only RGB crops.

B. Knowledge Distillation

Our training objective combines soft supervision from the teacher model with hard supervision from ground truth masks. Specifically, we use a two-part loss: (1) a mean squared error loss (\mathcal{L}_{MSE}) to match the teacher’s soft logits [31], and (2) a dual-component alignment loss consisting of balanced binary cross-entropy (\mathcal{L}_{BCE}) and Dice loss (\mathcal{L}_{Dice}) [29], [32]. The total loss is:

$$\mathcal{L}_{total} = \lambda \cdot \mathcal{L}_{MSE} + (1 - \lambda) \cdot (0.5 \mathcal{L}_{BCE} + 0.5 \mathcal{L}_{Dice}) \quad (1)$$

where $\lambda \in (0, 1)$ is dynamically adjusted based on the confidence of the teacher [33], allowing the student to rely more heavily on the teacher when the predictions are reliable and on the ground truth otherwise.

C. Training, Quantization and Deployment

The student model was trained on COCO [34] using the AdamW optimizer [35] and evaluated on LVIS [36]. After training, we perform static quantization to INT8 [37]–[42]. For hardware benchmarking, we used the Sony IMX500 intelligent vision sensor [7], [8], a stacked BSI-CMOS image sensor with an integrated DSP optimized for CNN inference. The sensor features 2304 MAC units and a 262.5MHz programmable DSP capable of 4.97 TOPS/W. CNN results were transmitted via the SPI interface, enabling a low-power, compact edge deployment, demonstrating that promptable segmentation can run in-sensor under tight memory and operator constraints.

TABLE I: Comparison of Edge Segmentation Models. Latencies were measured on a NVIDIA T4 instance, except Q-PicoSAM2 (*) which is on the Sony IMX500.

Model	MACs ↓	Latency ↓	COCO mIoU ↑	LVIS mIoU ↑	Params (M) ↓	Size (MB) ↓	IMX500
SAM-H	2.97T	2.39 s	53.6	60.5	635	2420.3	✗
FastSAM	443G	153.6 ms	51.6	55.2	72.2	275.6	✗
TinySAM	42G	38.4 ms	50.9	52.1	9.7	37.0	✗
EdgeSAM	42G	38.4 ms	48.0	53.7	9.7	37.0	✗
LiteSAM	4.2G	16.0 ms	49.0	51.2	4.2	16.0	✗
Supervised	336M	2.5 ms	53.0	41.4	1.3	4.87	✓
PicoSAM2	336M	2.54 ms	51.9	44.9	1.3	4.87	✓
Q-PicoSAM2	324M	14.3 ms*	50.5	45.1	1.3	1.22	✓

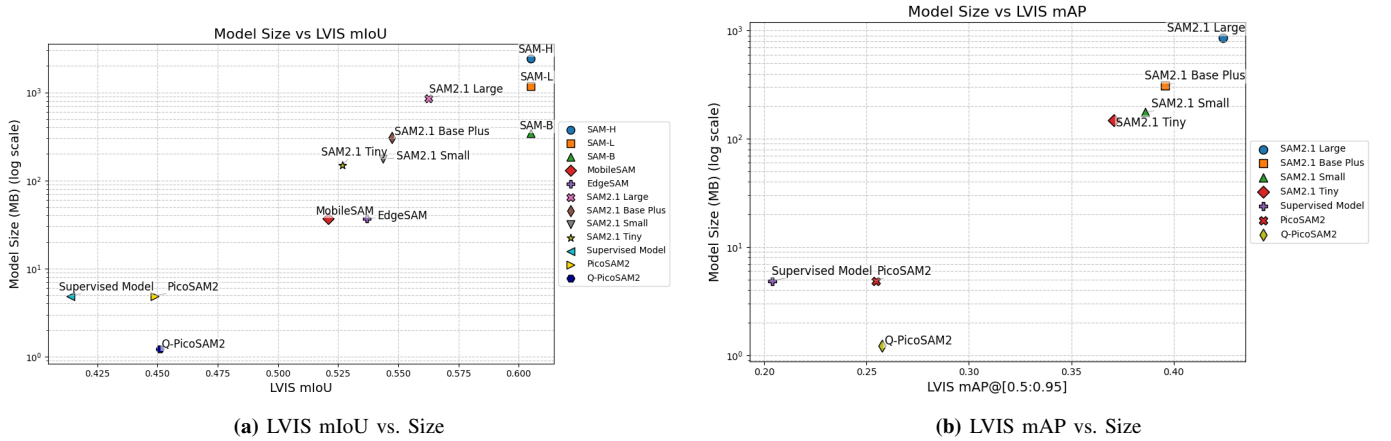


Fig. 4: Segmentation accuracy (mIoU) and precision (mAP) vs. model size on LVIS (log scale).

IV. EXPERIMENTAL RESULTS

PicoSAM2 was benchmarked against lightweight segmentation models across compute cost, accuracy, and deployability. Table I summarizes MACs, latency, mIoU on COCO/LVIS, model size, and IMX500 compatibility.

PicoSAM2 achieves the lowest compute cost at 336M MACs and an inference latency of 2.54ms on an NVIDIA T4 GPU. Q-PicoSAM2 runs at 14.3ms inference latency on the Sony IMX500. Based on this, it achieves approximately 86 MACs per cycle on the IMX500. It is also the only segmentation model to satisfy the strict < 8 MB memory constraint (1.3M parameters, 1.22MB quantized). Despite these constraints, it delivers 51.9% mIoU on COCO and 44.9% on LVIS.

Distillation yields a boost of +3.5% mIoU and +5.1% mAP in LVIS versus standard training. Figure 1 illustrates the trade-off between latency and model size on a logarithmic scale, highlighting the position of PicoSAM2 at the lowest latency and smallest size among all models compared. PicoSAM2 achieves strong segmentation accuracy (mIoU) on COCO and LVIS datasets relative to its size (see Figure 4a). The distilled PicoSAM2 model significantly improves precision in LVIS compared to the supervised baseline (see Figure 4b).

The qualitative comparisons in Figure 2 show that PicoSAM2 produces high-quality single-prompt segmentation masks, thanks to its task-specific design.

V. CONCLUSION & DISCUSSION

This work introduces PicoSAM2, a prompt-based segmentation model tailored for real-time deployment on the Sony IMX500 edge AI vision sensor. By rethinking the design of segmentation architectures for extreme efficiency, PicoSAM2 achieves competitive performance in three core dimensions: computational cost, segmentation accuracy, and deployability. In terms of compute, PicoSAM2 operates with just 336M MACs—less than 0.02% of SAM-H—and achieves real-time performance with 2.5 ms GPU latency and 14.3 ms on-device latency after INT8 quantization. Despite its small footprint (1.3M parameters and 1.22 MB quantized), the model retains strong performance with 51.9% mIoU on COCO and 45.1% on LVIS using a single-point prompt. Crucially, it meets the IMX500’s stringent 8 MB memory restriction, operates with input only in RGB, and complies with limited ONNX operator support. Notably, Q-PicoSAM2 achieves an inference efficiency of approximately 86 MACs per cycle on the Sony IMX500 when accounting for the model inference. Ablation studies confirm that SAM2 distillation improves generalization over purely supervised learning (+5.08% mAP on LVIS), validating the benefits of hybrid supervision under limited data regimes. In addition, fixed spatial prompting enables the model to remain promptable even under severe modality constraints, although with limitations in flexibility and interpretability. This work demonstrates the viability of deploying intelligent, prompt-based vision models directly on constrained sensors.

REFERENCES

- [1] A. Kirillov, E. Mintun, N. Ravi, H. Mao, C. Rolland, L. Gustafson, T. Xiao, S. Whitehead, A. C. Berg, W.-Y. Lo, P. Dollár, and R. Girshick, "Segment anything," 2023.
- [2] N. Ravi, V. Gabeur, Y. Hu, R. Hu, C. Ryali, T. Ma, H. Khedr, R. Rädle, C. Rolland, L. Gustafson, E. Mintun, J. Pan, K. V. Alwala, N. Carion, C. Wu, R. Girshick, P. Dollár, and C. Feichtenhofer, "Sam2: Segment anything in images and videos," *arXiv preprint arXiv:2408.00714*, 2024.
- [3] J. Lin, W.-M. Chen, Y. Lin, C. Gan, S. Han *et al.*, "McuNet: Tiny deep learning on iot devices," *Advances in Neural Information Processing Systems*, vol. 33, pp. 11 711–11 722, 2020.
- [4] X. Wang, M. Magno, L. Cavigelli, and L. Benini, "Fann-on-mcu: An open-source toolkit for energy-efficient neural network inference at the edge of the internet of things," *IEEE Internet of Things Journal*, vol. 7, no. 5, pp. 4403–4417, 2020.
- [5] M. Giordano, L. Piccinelli, and M. Magno, "Survey and comparison of milliwatts micro controllers for tiny machine learning at the edge," in *2022 IEEE 4th International Conference on Artificial Intelligence Circuits and Systems (AICAS)*. IEEE, 2022, pp. 94–97.
- [6] J. Moosmann, P. Bonazzi, Y. Li, S. Bian, P. Mayer, L. Benini, and M. Magno, "Ultra-efficient on-device object detection on ai-integrated smart glasses," 2023.
- [7] "Sony imx500," 2023. [Online]. Available: <https://developer.sony.com/imx500/>
- [8] R. Eki, S. Yamada, H. Ozawa, H. Kai, K. Okuike, H. Gowtham, H. Nakanishi, E. Almog, Y. Livne, G. Yuval, E. Zyss, and T. Izawa, "A 1/2.3inch 12.3mpixel with on-chip 4.97tops/w cnn processor back-illuminated stacked cmos image sensor," in *2021 IEEE International Solid-State Circuits Conference (ISSCC)*. IEEE, 2021, pp. 154–155.
- [9] P. Bonazzi, T. Rüegg, S. Bian, Y. Li, and M. Magno, "Tinytracker: Ultra-fast and ultra-low-power edge vision for in-sensor gaze estimation," pp. 1–4, 2023.
- [10] F. Zhou and Y. Chai, "Near-sensor and in-sensor computing," *Nature Electronics*, vol. 3, no. 11, pp. 664–671, 2020.
- [11] H. Shu, W. Li, Y. Tang, Y. Zhang, Y. Chen, H. Li, Y. Wang, and X. Chen, "Tinsam: Pushing the envelope for efficient segment anything model," *arXiv preprint arXiv:2312.13789*, 2023, also available via AAAI implementation.
- [12] C. Zhou, X. Li, C. C. Loy, and B. Dai, "Edgesam: Prompt-in-the-loop distillation for on-device deployment of sam," *arXiv preprint arXiv:2312.06660*, 2023.
- [13] C. Zhang, D. Han, S. Zheng, J. Choi, T. Kim, and C. S. Hong, "Mobilesamv2: Faster segment anything to everything," *arXiv preprint arXiv:2312.09579*, 2023.
- [14] J. Fu, Y. Yu, N. Li, Y. Zhang, Q. Chen, J. Xiong, J. Yin, and Z. Xiang, "Lite-sam is actually what you need for segment everything," in *European Conference on Computer Vision (ECCV)*, 2024, *arXiv preprint arXiv:2407.08965*.
- [15] M. Guo, L. Zhang, and Y. Sun, "Fastsam: Faster segment anything model," *arXiv preprint arXiv:2304.12345*, 2023.
- [16] H. Chen, L. Xu, and W. Zhang, "Mobilesam: Efficient promptable segmentation for mobile devices," *arXiv preprint arXiv:2306.04567*, 2023.
- [17] M. Li, Q. Gao, and H. Xu, "Efficientsam: An efficient segment anything model via architecture redesign," *arXiv preprint arXiv:2402.01122*, 2024.
- [18] L. Zhang, W. Sun, and J. Huang, "Efficientvit-sam: Combining vision transformers and efficient architectures for segmentation," *arXiv preprint arXiv:2403.02233*, 2024.
- [19] Y. Liu, Z. Wang, and F. Chen, "Repvit-sam: Re-parameterized vision transformer for segment anything," *arXiv preprint arXiv:2404.06789*, 2024.
- [20] K. Wang, Y. Zhao, and L. Chen, "Sam-lightening: Pruning and quantization for lightweight sam models," *arXiv preprint arXiv:2405.03456*, 2024.
- [21] J. Kim, M. Park, and S. Lee, "Slimsam: Model pruning for efficient visual segmentation," *arXiv preprint arXiv:2401.04567*, 2024.
- [22] S. Park, H. Choi, and D. Jung, "Expedit-sam: Training-free optimization for promptable segmentation," *arXiv preprint arXiv:2403.08901*, 2024.
- [23] X. Zhao, W. Ding, Y. An, Y. Du, T. Yu, M. Li, M. Tang, and J. Wang, "Fast segment anything," 2023.
- [24] R. Banner, I. Hubara, E. Hoffer, and D. Soudry, "Post training 4-bit quantization of convolutional networks for rapid-deployment," in *Advances in Neural Information Processing Systems (NeurIPS)*, vol. 32, 2019.
- [25] M. Nagel, M. van Baalen, T. Blankevoort, and M. Welling, "Up or down? adaptive rounding for post-training quantization," in *European Conference on Computer Vision (ECCV)*. Springer, 2020, pp. 216–233.
- [26] A. Vasudevan, M. Dehghani, A. Kolesnikov, L. Beyer, X. Zhai, and N. Houlsby, "HierA: A hierarchical vision transformer without the bells-and-whistles," *arXiv preprint arXiv:2306.00989*, 2023.
- [27] H. Wang, K. Wang, Y. Xu, C. Xu, and C. Shen, "Litevit: Towards efficient vision transformers with enhanced token mixing," *arXiv preprint arXiv:2303.13429*, 2023.
- [28] Y. Xu, F. Yu, and B. Zhou, "Autopppn: Learning to design promptable pyramid networks for efficient segmentation," in *Proceedings of the IEEE/CVF International Conference on Computer Vision (ICCV)*, 2023, pp. 21 228–21 238.
- [29] O. Ronneberger, P. Fischer, and T. Brox, "U-Net: Convolutional networks for biomedical image segmentation," in *MICCAI*, 2015, pp. 234–241.
- [30] F. Chollet, "Xception: Deep learning with depthwise separable convolutions," in *CVPR*, 2017.
- [31] G. Hinton, O. Vinyals, and J. Dean, "Distilling the knowledge in a neural network," *arXiv preprint arXiv:1503.02531*, 2015.
- [32] F. Milletari, N. Navab, and S. Ahmadi, "V-net: Fully convolutional neural networks for volumetric medical image segmentation," *3DV*, 2016.
- [33] V. Sanh, L. Debut, J. Chaumond, and T. Wolf, "Distilbert, a distilled version of bert: smaller, faster, cheaper and lighter," *ArXiv*, vol. abs/1910.01108, 2019.
- [34] T.-Y. Lin, M. Maire, S. Belongie, L. Bourdev, R. Girshick, J. Hays, P. Perona, D. Ramanan, C. L. Zitnick, and P. Dollár, "Microsoft coco: Common objects in context," *arXiv preprint arXiv:1405.0312*, 2014.
- [35] I. Loshchilov and F. Hutter, "Decoupled weight decay regularization," in *International Conference on Learning Representations (ICLR)*, 2019.
- [36] A. Gupta, P. Dollar, and R. Girshick, "Lvis: A dataset for large vocabulary instance segmentation," in *Proceedings of the IEEE/CVF Conference on Computer Vision and Pattern Recognition (CVPR)*, 2019.
- [37] A. Gholami, S. Kim, Z. Dong, Z. Yao, M. W. Mahoney, and K. Keutzer, "A survey of quantization methods for efficient neural network inference," 2021. [Online]. Available: <https://arxiv.org/abs/2103.13630>
- [38] H. V. Habi, R. Peretz, E. Cohen, L. Dikstein, O. Dror, I. Diamant, R. H. Jennings, and A. Netzer, "Hptq: Hardware-friendly post training quantization," *arXiv preprint arXiv:2109.09113*, 2021.
- [39] O. Gordon, E. Cohen, H. V. Habi, and A. Netzer, "Eptq: Enhanced post-training quantization via hessian-guided network-wise optimization," in *ECCV Workshops (11)*, 2024.
- [40] L. Dikstein, A. Lapid, A. Netzer, and H. V. Habi, "Data generation for hardware-friendly post-training quantization," in *IEEE/CVF Winter Conference on Applications of Computer Vision (WACV)*, 2025.
- [41] PyTorch Team, *torchvision.models*, <https://pytorch.org/vision/stable/models.html>.
- [42] Keras Team, *Keras Applications*, <https://keras.io/api/applications/>.